# Selective Detection of Trace $Cr^{3+}$ in Aqueous Solution by Using 5,5′-Dithiobis (2-Nitrobenzoic acid)-Modified Gold Nanoparticles

**Yong-Qiang Dang, Hong-Wei Li, Bin Wang, Lei Li, and Yuqing Wu***

State Key Laboratory of Supramolecular Structure and Materials, No. 2699 Qianjin Street, Jilin University, Changchun 130012, China

**ABSTRACT** A simply prepared gold nanoparticle-based sensor, 5,5′-dithiobis (2-nitrobenzoic acid) (DTNBA)-modified gold nanoparticles, was prepared to explore the sensitive and selective detection of metal ions using a colorimetric technique. The selective detection of trace levels (93.6 ppb) $Cr^{3+}$ in aqueous solution was achieved over 15 other metal ions. The functionalized gold nanoparticles became aggregated in solution in the presence of $Cr^{3+}$ by an ion-templated chelation process, which caused an easily measurable change in the extinction spectrum of the particles and provided an inherently sensitive method for $Cr^{3+}$ detection in aqueous solution.

**KEYWORDS:** gold nanoparticles • DTNBA • colorimetric • ion detection • chromium

## 1. INTRODUCTION

The development of highly sensitive and selective analytical methodology for the detection of trace levels of chromium species is of significant interest. In aqueous solution, chromium often exists in two oxidation states, chromium(III) and chromium(VI) (1). And $Cr^{3+}$ generally has ambivalent functions for humans (2−5): $Cr^{3+}$ is an essential trace element in human nutrition, which has great impact on the metabolism of carbohydrates, fats, proteins, and nucleic acids by activating certain enzymes and stabilizing proteins and nucleic acids. On the other hand, high levels of $Cr^{3+}$ can bind to DNA, negatively affecting cellular structures and damaging the cellular components, although its toxicity observed in vivo is less serious than that of $Cr^{6+}$. Therefore, under the strict rules for human health, it becomes an important goal to explore new chromium detection methods that are effective, rapid, and applicable to the environmental and biological systems. However, it remains a challenge to date. Few other direct determinations of chromium in water have been carried out except traditional analytical methods as inductively coupled plasma-atomic emission spectrometry or electrothermal atomic absorption spectrometry (2, 6−8), procedures that generally are time-consuming, expensive, and/or inconvenient to perform. Several fluorescent chemosensors for $Cr^{3+}$ have been reported recently, but they require using organic solvents and generally have a relatively high detection limit (5, 9). Herein, we report a simply prepared gold nanoparticle-based sensor for detecting $Cr^{3+}$ over 15 other metal ions including chromium(VI) in aqueous solution.

Metal nanoparticles are emerging as important colorimetric reporters because their extremely high visible-region extinction coefficients ($1 \times 10^8$ to $1 \times 10^{10}$ $M^{-1}$ $cm^{-1}$) are often several orders of magnitude higher than that of organic dyes. In recent years, gold nanoparticles have been extensively used for the detection of metal ions through the aggregation/isolation of the particles (10−14). Obare et al. used 2,9-dibutyl-1,10-phenanthroline-5,6-aminoethanethiol-modified gold nanoparticles to specifically detect $Li^+$ in aqueous solution (12). Yoosaf et al. developed a method to synthesize gold nanoparticles capped with gallic acid in situ and to detect micromolar quantities $Pb^{2+}$ ions in the presence of other metal cations (13). Huang et al. unveiled a mercaptopropionic acid-modified gold nanoparticles in the presence of 2,6-pyridinedicarboxylic acid for the highly selective and sensitive detection of $Hg^{2+}$ in aqueous solution (14). Thus, gold nanoparticles modified by appropriate small functional molecules can be used to detect metal ions in aqueous solution with good selectivity and sensitivity. In addition, although other studies utilizing gold nanoparticles to detect different ions have recently been reported with improved selectivity and sensitivity, these systems have been generally more complex (15−21). To the best of our knowledge, small molecule-modified gold nanoparticles in aqueous solution have not yet been used for the detection of carcinogenic $Cr^{3+}$. In the present investigation, we describe gold nanoparticles modified with a frequently used functional molecule, 5,5′-dithiobis (2-nitrobenzoic acid) (DTNBA), which displays binding sites for metal ions in aqueous solution.

DTNBA, also called Ellman's reagent, is one of the most widely used colorimetric agents for the detection of thiols

* Corresponding author. Fax: 86-431-85193421. Tel: 86-431-85168730. E-mail: yqwu@jlu.edu.cn.
Received for review March 23, 2009 and accepted May 31, 2009

DOI: 10.1021/am9001953

in biological samples (22−24). It can react with 2 equiv. of free thiol species (R-SH) to form the disulfide group (RSSR) and 2 equiv. of the highly colored 5-thio-2-nitrobenzoic acid (TNBA) species. Therefore, when mixed with gold nanoparticles, the disulfide group in DTNBA can easily break and form an Au−S bond. Meanwhile, the nitryl and carboxyl moieties linked with the phenyl ring have good properties of hydrophilicity and nucleophilicity, affording a good expectation of their usefulness in the binding of metal ions. By adding DTNBA to gold nanoparticles in solution, we obtained functionalized nanostructures, TNBA-modified gold nanoparticles (TNBA-AuNPs). These TNBA-AuNPs aggregated specifically upon the addition of $Cr^{3+}$ in a highly sensitive manner in aqueous solution.

This gold nanoparticle-based sensor has several advantages, including (i) simple and low-cost preparation; (ii) high selectivity and sensitivity to $Cr^{3+}$ with a detection limit of 93.6 ppb; (iii) displaying a marked red-shift in the UV−vis extinction spectra and a visible color change from pink to blue; and (iv) detection of $Cr^{3+}$ in aqueous solution, excluding the need for any organic solvent.

## 2. EXPERIMENTAL SECTION

**2.1. Chemicals.** Hydrogen tetrachloroaurate ($HAuCl_4 \cdot 3H_2O$), 5,5′-dithiobis (2-nitrobenzoic acid) (DTNBA), 2-nitrobenzoic acid (NBA), 3-mercaptobenzoic acid (MBA), HEPES, and sodium citrate were purchased from Sigma-Aldrich and used without further purification. The synthesis and characterization of dimethyl 5,5′-dithiobis (2-nitrobenzoate) (DTNB-OMe) are described in the Supporting Information.

**2.2. Gold Nanoparticle Synthesis.** Gold nanoparticles with diameters 13 nm were prepared through the citrate-mediated reduction of $HAuCl_4$ (25−27). Briefly summarized, an aqueous solution of 0.3 mM $HAuCl_4$ (100 mL) was brought to a vigorous boil with stirring in a round-bottom flask fitted with a reflux condenser; 1% sodium citrate (5 mL) was then added rapidly to the solution. The solution was heated under reflux for another 15 min, during which time its color changed from pale yellow to deep red. The solution was cooled to room temperature while stirring continuously. The nanoparticles were characterized by transmission electron microscopy (TEM) and UV−visible absorption spectroscopy. The particle concentration of the AuNPs (ca. 11.25 nM) was determined according to Beer's law using the molar extinction coefficient of ca. $1 \times 10^8$ $M^{-1}cm^{-1}$ at 520 nm for AuNPs of 13.3 nm diameter, as reported (14).

**2.3. Modification of Gold Nanoparticles.** TNBA-AuNPs and MBA-AuNPs were prepared by adding 10.0 mM DTNBA (pH 7.5) or 10.0 mM MBA in different volumes to the as-prepared 13-nm-diameter AuNPs solution (11.25 nM; 20 mL) with stirring overnight. Then the mixture was centrifuged for 10 min at 9562.5 g, and the deposition was washed three times by water. The pellet was diluted to 1.5 nM with 10.0 mM HEPES buffer solution. DTNB-OMe was dissolved in THF (5 mM), and TNB-OMe-AuNPs was prepared using the same method as above.

**2.4. Equipment.** UV−visible extinction spectrum was measured on a SHIMADZU UV-3600 spectrophotometer. TEM images were acquired on a Hitachi H-8100IV electron microscope at 200 kV. Samples were prepared by placing a drop of the colloidal solution onto a Formvar-coated copper grid. The zeta-potential measurement was performed using a Zetasizer Nano ZS (Malvern Instruments). Because of the uncertainties of zeta-potential measurements, each sample was measured five times and the average data were reported.

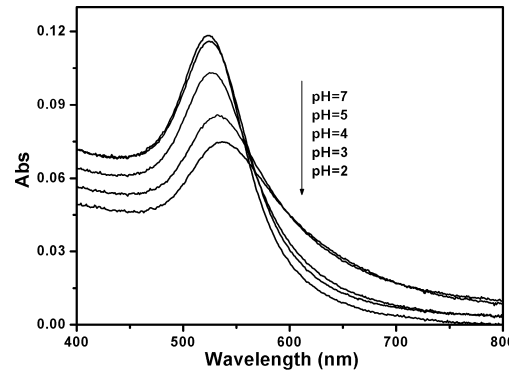


**FIGURE 1. UV−visible extinction spectra of TNBA-AuNPs with 10 min incubation after adjusting to the destination pH values.**

**Table 1. ζ Potential of TNBA-AuNPs at Different pH Values**

| pH | zeta potential (mV) |
|---|---|
| 8.0 | −51.1 ± 2.3 |
| 7.0 | −49.9 ± 4.7 |
| 6.0 | −44.4 ± 3.0 |
| 5.0 | −9.8 ± 0.5 |
| 4.0 | 5.9 ± 0.8 |

## 3. RESULTS AND DISCUSSION

**3.1. Stability of TNBA-AuNPs.** Gold nanoparticles prepared by the described process displayed an extinction band at 520 nm. When the preparation was modified by TNBA, the extinction band shifted from 520 to 524 nm (see Figure S1 in the Supporting Information), as expected for the surface thiolation of nanoparticles (12). The slight shift in wavelength may also be attributed to the centrifugation of the ligand-modified Au particles, a factor that sometimes affects the size distribution (28). We examined the effect of pH on the UV−visible extinction spectra of the prepared TNBA-AuNPs (Figure 1). When the pH is higher than 6.0, the TNBA-AuNPs solution was stable over 1 week. However, when the pH is lower than 5.0, with time a slight red-shift of the extinction band and modest precipitation were observed. To understand this outcome better, we measured the zeta potential (ζ) of the TNBA-AuNPs at different pH values (Table 1). Colloidal particles having a ζ value higher than +30 mV or lower than −30 mV are generally regarded as stable because of the strong electrostatic repulsion between the particles, which prevents them from aggregation (14). The results in Table 1 illustrate that pH values higher than 6.0 were conducive to stable TNBA-AuNPs in solution, whereas at a pH of 5.0 and lower, TNBA-AuNPs possessed low ζ values where the carboxylic groups of TNBA may exist in its neutral form, resulting in a weak surface interaction and unstable TNBA-AuNPs in solution. These results are consistent with those obtained from UV−visible extinction spectra in Figure 1.

**3.2. Optimization of the Responsive Condition of TNBA-AuNPs to $Cr^{3+}$ in Solution.** Because the nanoparticles are stable in the pH range greater than 6.0,

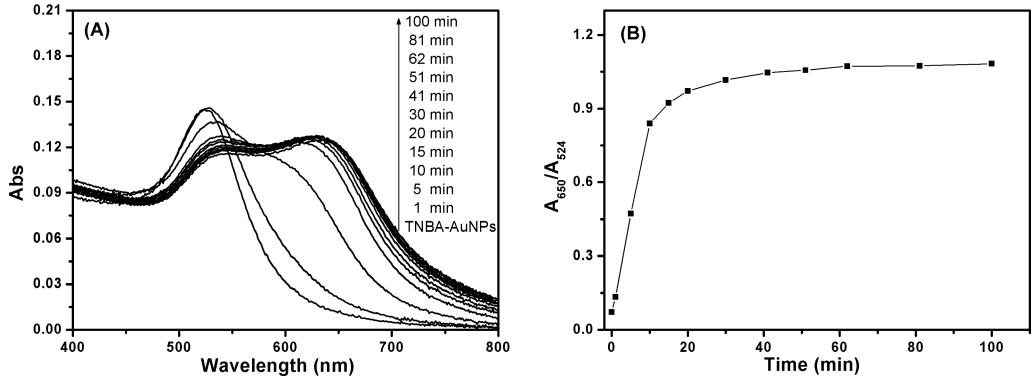


**FIGURE 2. Time-course measurements of (A) UV−vis extinction spectra and (B) $A_{650}/A_{524}$ for TNBA-AuNPs after the addition of $Cr^{3+}$ (10.0 $\mu$M).**

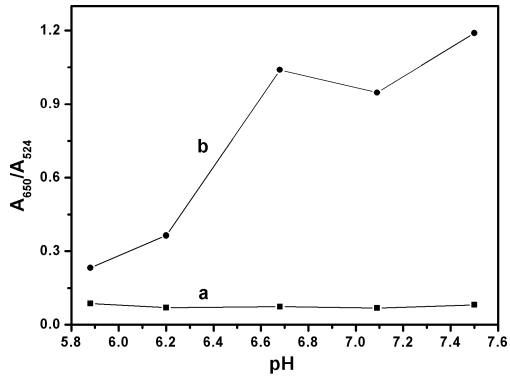


**FIGURE 3. pH-Dependent response profiles of the extinction intensity ratio $A_{650}/A_{524}$ of TNBA-AuNPs (a) before and (b) after mixing with $Cr^{3+}$ (3.0 $\mu$M).**

we conducted studies of their binding with metal ions using 10.0 mM HEPES buffer solution, pH 7.5. We tested the practicality of the TNBA-AuNPs solution for sensing of various metal ions by observing the UV−vis extinction spectra. In the presence of $Cr^{3+}$, TNBA-AuNPs displayed a red-shift of the extinction band. This spectral change, which can be characterized by the ratio of the extinction band intensity of the aggregated to the isolated forms ($A_{650}/A_{524}$), increased with time. Figure 2 displays the time-dependent changes in the UV−vis extinction spectra of the TNBA-AuNPs after the addition of 10.0 $\mu$M $Cr^{3+}$. After 30 min, the $Cr^{3+}$-induced change of $A_{650}/A_{524}$ had almost reached its maximum (Figure 2B). Therefore, after the addition of metal ions, 30 min incubation time was chosen for further detection studies.

As the functional group of TNBA is sensitive to pH, we also optimized the responsive pH of TNBA-AuNPs to $Cr^{3+}$ around neutral pH (pH 5.8−7.5) (Figure 3). A highly sensitive response of the value of $A_{650}/A_{524}$ was achieved over the pH range of 6.5−7.5, in which most of the metal ions were satisfactorily stable. In all subsequent experiments, we used 10.0 mM HEPES buffer to keep the pH value at 7.5.

We also investigated the optimum TNBA density on the gold nanoparticle surfaces for the binding of $Cr^{3+}$ in solution. The calibration curves of $Cr^{3+}$ in various TNBA-AuNPs solutions are shown in Figure S2 of the Supporting Information. We noted that TNBA density higher than 2000 on a TNBA-AuNP surface did not induce notable differences in the calibration curves for $Cr^{3+}$, whereas a TNBA density lower than 2000 would be less efficient because it showed a relatively higher responsive concentration range for $Cr^{3+}$. This effect may be due to a smaller TNBA population on the surface. But all of the TNBA-AuNP preparations changed over a narrow concentration range of $Cr^{3+}$ (1−5 $\mu$M), this result would not significantly influence the detection of $Cr^{3+}$ in practical applications. Therefore, in all the following studies, the maximally modified TNBA-AuNPs were employed for the detection of metal ions.

**3.3. Selective Detection of TNBA-AuNPs for $Cr^{3+}$ and Other Metal Ions.** Figure 4A displays the UV−vis extinction spectra of the TNBA-AuNPs solution before and after adding various metal ions (5.0 $\mu$M) for 30 min. In this series of studies, the presence of $Cr^{3+}$ led to a marked red-shift of extinction bands, whereas the presence of $Pb^{2+}$, $Al^{3+}$, and other ions led to only minor red-shifts of the extinction band. The sensitivity and selectivity of nanoparticles toward various metal ions at pH 7.5 were further quantified by plotting the extinction intensity ratio ($A_{650}/A_{524}$) of TNBA-AuNPs solution at a fixed concentration of metal ions (5.0 $\mu$M) (Figure 4B). The $Cr^{3+}$-induced value of $A_{650}/A_{524}$ was ~17-fold larger than those achieved by other metal ions, which indicated that the value of $A_{650}/A_{524}$ can be used to display the distinctive interaction between TNBA-modified gold nanoparticles and $Cr^{3+}$. In addition, the marked bathochromic shift ($\Delta\lambda_{MAX}$ = 125 nm) of the extinction band and the augmentation of the value of $A_{650}/A_{524}$ induced by $Cr^{3+}$ in TNBA-AuNPs solution can be seen by the naked eye, with the color of the TNBA-AuNPs changing from pink to blue after 30 min incubation. After 5 h, it led to precipitation of the TNBA-AuNPs. The color changes of the TNBA-AuNPs solutions with different metal ions are illustrated in the insert of Figure 4B. The discrimination of TNBA-AuNPs for $Cr^{3+}$ as opposed to other metal ions was revealed by the different colors.

To investigate the band shift and color change of the TNBA-AuNPs in solution induced by the addition of $Cr^{3+}$, we also performed a TEM study on these particles in the absence and presence of $Cr^{3+}$ (5.0 $\mu$M) (Figure 5). We proposed that the large band shift ($\Delta\lambda_{MAX}$ = 125 nm, as shown in Figure 4A) in the extinction band of TNBA-AuNPs may indicate strong aggregation of particles (12−14). From the TEM

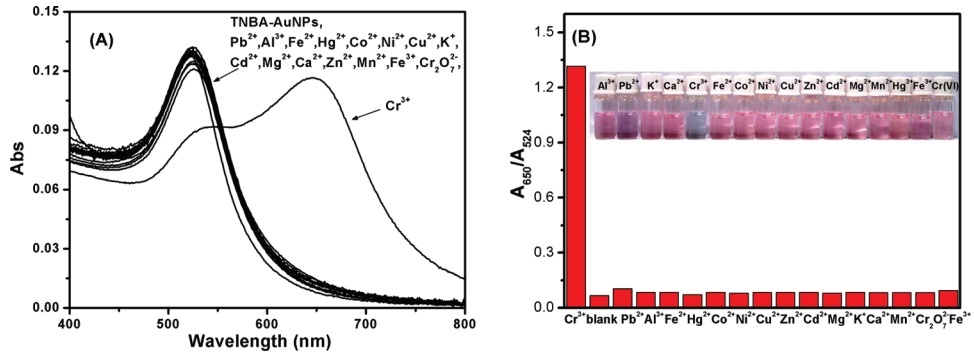


FIGURE 4. (A) UV−visible extinction profile of TNBA-AuNPs (1.5 nM) before and after the addition of different kinds of metal ions (5.0 $\mu$M). (B) Value of $A_{650}/A_{524}$ and photographic images of TNBA-AuNPs (1.5 nM) in the presence of different metal ions (5.0 $\mu$M) in 10.0 mM HEPES buffer (pH 7.5).

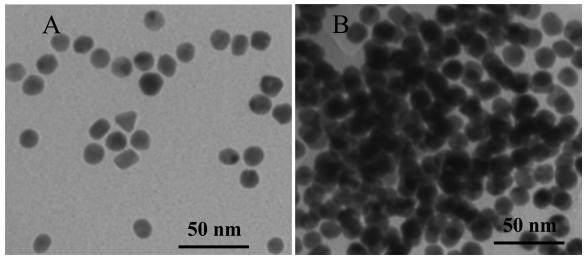


FIGURE 5. TEM images of TNBA-AuNPs solution in the (A) absence and (B) presence of $Cr^{3+}$ ions (5.0 $\mu$M).

images of TNBA-AuNPs in solution (Figure 5), we observed the aggregation of the TNBA-AuNPs in the presence of $Cr^{3+}$ (5.0 $\mu$M). In accordance with the general coordination number of 6 for $Cr^{3+}$ (5), we assumed that at least two TNBA which were bound to different nanoparticles could interact with $Cr^{3+}$ through chelation and/or electrostatic interactions. This interaction between $Cr^{3+}$ and TNBA may be strong enough to overcome the electrostatic repulsion imposed by TNBA-AuNPs (13), thus inducing particle aggregation.

**3.4. Responsive Sensitivity of TNBA-AuNPs to $Cr^{3+}$ in Buffer Solution.** With the addition of $Cr^{3+}$, the extinction band of TNBA-AuNPs changed gradually from 524 nm to longer wavelengths, finally reached a maximum of 650 nm (Figure 6A). To quantitatively describe the responsive sensitivity and selectivity of TNBA-AuNPs toward various metal ions at pH 7.5, we plotted the ratio of $A_{650}/A_{524}$ against the concentration of different metal ions, respectively (Figure 6B). From the ratiometric plots, it is clear that the concentration of $Cr^{3+}$ higher than 1.8 $\mu$M (i.e., 93.6 ppb) can induce the interparticle association of TNBA-AuNPs, leading to an obvious red-shift of the extinction band. However, no obvious extinction band at 650 nm was observed with other metal ions such as $Cd^{2+}$, $Cu^{2+}$, $Zn^{2+}$, and $Ni^{2+}$, even at concentration as high as 20 $\mu$M. Only $Pb^{2+}$ had a slight effect when its concentration higher than 7.5 $\mu$M (Figure 6B). Therefore, the TNBA-AuNPs displayed selective detection of trace $Cr^{3+}$ in aqueous solution over 15 other metal ions.

To further clarify the selectivity of TNBA-AuNPs toward $Cr^{3+}$ in solution, we measured the UV−vis absorption spectra of sole DTNBA upon addition of $Cr^{3+}$ and other different metal ions, respectively. It was observed that the addition of $Cr^{3+}$ (Figure 7A) and $Pb^{2+}$ (see Figure S3A in the Supporting Information) led to a minor blue-shift and an increase in the absorption band of DTNBA, which may be due to the change of charge density on the phenyl ring upon the strong binding of linked nitryl and carboxyl groups to these two metal ions. The binding behavior of DTNBA toward other metal ions did not induce obvious changes of their absorption bands (see Figure S3B in the Supporting Information), except $Fe^{2+}$ and $Fe^{3+}$, which induced marked shifts and increases in absorption band of DTNBA. Further investigation on the absorption responses of 2-nitrobenzoic acid (NBA) to $Cr^{3+}$, $Pb^{2+}$, and other different metal ions was also taken to exclude the effect of disulfide bond. And the

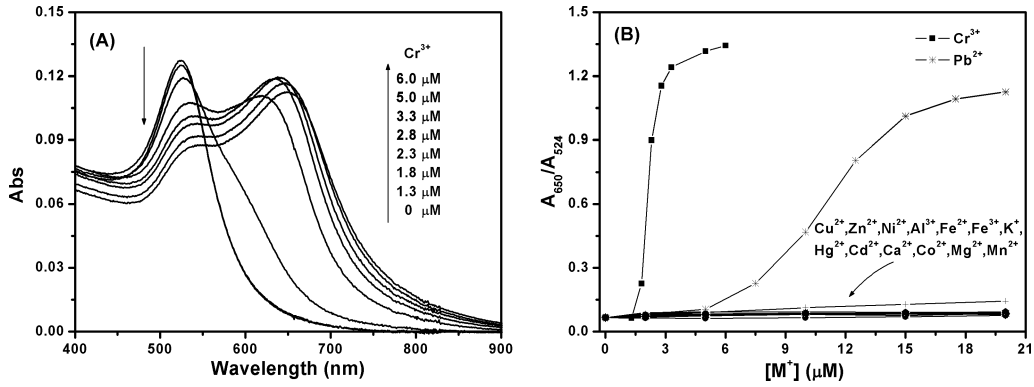


FIGURE 6. (A) UV−vis extinction spectra of TNBA-AuNPs before and after addition of different concentrations of $Cr^{3+}$, and (B) responses of $A_{650}/A_{524}$ as a function of the concentration of different metal ion, respectively.

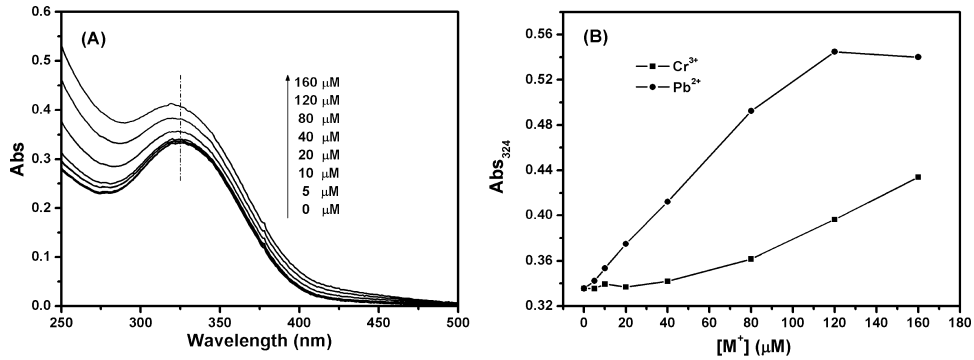


**FIGURE 7. (A) UV−vis absorption spectra of 20 $\mu$M DTNBA upon addition of $Cr^{3+}$ in 10.0 mM HEPES buffer aqueous solutions (pH 7.5), and (B) responses of absorption at 324 nm as a function of the concentration of $Cr^{3+}$ and $Pb^{2+}$.**

results confirmed that the nitryl and carboxyl groups linked to the phenyl ring selectively interacted with $Cr^{3+}$ because similar minor blue-shift and increase of absorption band of NBA were observed with the addition of $Cr^{3+}$ or $Pb^{2+}$ (see Figure S4A−C in the Supporting Information). Therefore, it can be concluded that the specific recognition of NBA moiety to $Cr^{3+}$ contributed greatly to the highly selective and sensitive response of TNBA-AuNPs to this ion. Of note was that although both DTNBA and NBA had stronger UV−vis absorption responses to $Pb^{2+}$ than to $Cr^{3+}$ in buffered aqueous solution (Figure 7B and Figure S4D in the Supporting Information), the functionalized gold nanoparticles, TNBA-AuNPs, displayed much sensitive response to $Cr^{3+}$ than that to $Pb^{2+}$ by an ion-templated aggregation.

In addition, to further reveal the contribution of nitryl or carboxyl group separately to the selective detection of TNBA-AuNPs to $Cr^{3+}$, we employed two analogues of TNBA, 3-mercaptobenzoic acid (MBA) and dimethyl 5,5′-dithiobis (2-nitrobenzoate) (DTNB-OMe) to modify the gold nanoparticles. The UV−vis extinction spectra of MBA-AuNPs and TNB-OMe-AuNPs upon addition of $Cr^{3+}$ and other different metal ions illustrated that MBA-AuNPs could aggregate in the presence of $Cr^{3+}$, $Pb^{2+}$, $Cd^{2+}$ and $Al^{3+}$ (see Figure S5 in the Supporting Information); but TNB-OMe-AuNPs could not aggregate even in the presence of 10 $\mu$M $Cr^{3+}$ (see Figure S6 in the Supporting Information). Therefore, it can be concluded that the carboxyl group plays a crucial role in the interaction of TNBA-AuNPs and $Cr^{3+}$, whereas the nitryl group contributes greatly to the selection of TNBA-AuNPs to $Cr^{3+}$.

## 4. CONCLUSIONS

In conclusion, in the present investigation, we have demonstrated a simply prepared chemosensor, which is sensitive and highly selective assay for $Cr^{3+}$ over 15 other metal ions in aqueous solution. The sensor is easily prepared by the functionalization of gold nanoparticles using DTNBA. The $Cr^{3+}$ chelation-induced aggregation of nanoparticles results in a marked red-shift ($\Delta\lambda_{MAX} = 125$ nm) in the UV−vis extinction band and a visible color change from pink to blue, which affords a sensitive detection of $Cr^{3+}$ with a detection limit of 93.6 ppb. Because the chemosensor was constructed on the basis of both the functional small molecule and gold nanoparticles, the selectivity and sensitivity of it could be improved by optimizing the structure of the capping ligand as well as the nanoparticle itself. We believe that the small molecule modified gold nanoparticles method has enormous potential for application with other toxic metal ion detection in biological and environmental samples.

**Acknowledgment.** The authors are grateful to the projects of NSFC (20773051), the Major State Basic Research Development Program (2007CB808006), the Programs for New Century Excellent Talents in University (NCET), and the 111 project (B06009).

**Supporting Information Available:** UV−vis spectra of AuNPs and TNBA-AuNPs comparison; those of DTNBA and NBA titrated by $Cr^{3+}$, $Pb^{2+}$ and other metal ions; and optimum TNBA density on the gold nanoparticle surfaces for the binding of $Cr^{3+}$ in solution (PDF). This material is available free of charge via the Internet at http://pubs.acs.org.

### REFERENCES AND NOTES

(1) Bagchi, D.; Stohs, S. J.; Downs, B. W.; Bagchi, M.; Preuss, H. G. *Toxicology* **2002**, *180*, 5–22.
(2) Hassanien, M. M.; Kenawy, I. M.; El-Menshawy, A. M.; El-Asmy, A. A. *J. Hazard. Mater.* **2008**, *158*, 170–176.
(3) Sun, Z.; Liang, P. *Microchim. Acta* **2008**, *162*, 121–125.
(4) Jena, B. K.; Raj, C. R. *Talanta* **2008**, *76*, 161–165.
(5) Zhou, Z.; Yu, M.; Yang, H.; Huang, K.; Li, F.; Yi, T.; Huang, C. *Chem. Commun.* **2008**, 3387–3389.
(6) Korn, M.; Korn, M. G.; Reis, B. F.; de Oliveira, E. *Talanta* **1994**, *41*, 2043–2047.
(7) Subramanian, K. S. *Anal. Chem.* **1988**, *60*, 11–15.
(8) Bednar, A. J.; Kirgan, R. A.; Jones, W. T. *Anal. Chim. Acta* **2009**, *632*, 27–34.
(9) Huang, K.; Yang, H.; Zhou, Z.; Yu, M.; Li, F.; Gao, X.; Yi, T.; Huang, C. *Org. Lett.* **2008**, *10*, 2557–2560.
(10) Cruz Enriquez, A.; Rivero Espejel, I. A.; Andrés García, E.; Díaz-García, M. E. *Anal. Bioanal. Chem.* **2008**, *391*, 807–815.
(11) Darbha, G. K.; Singh, A. K.; Rai, U. S.; Yu, E.; Yu, H.; Ray, P. C. *J. Am. Chem. Soc.* **2008**, *130*, 8038–8043.
(12) Obare, S. O.; Hollowell, R. E.; Murphy, C. J. *Langmuir* **2002**, *18*, 10407–10410.
(13) Yoosaf, K.; Ipe, B. I.; Suresh, C. H.; Thomas, K. G. *J. Phys. Chem. C* **2007**, *111*, 12839–12847.
(14) Huang, C. C.; Chang, H. T. *Chem. Commun.* **2007**, 1215–1217.
(15) Huang, C. C.; Chang, H. T. *Anal. Chem.* **2006**, *78*, 8332–8338.
(16) Tanaka, Y.; Oda, S.; Yamaguchi, H.; Kondo, Y.; Kojima, C.; Ono, A. *J. Am. Chem. Soc.* **2007**, *129*, 244–245.
(17) Liu, C. W.; Hsieh, Y. T.; Huang, C. C.; Lin, Z. H.; Chang, H. T. *Chem. Commun.* **2008**, 2242–2244.

(18) Huang, C. C.; Yang, Z.; Lee, K. H.; Chang, H. T. *Angew. Chem., Int. Ed.* **2007**, *46*, 6824–6828.
(19) Darbha, G. K.; Ray, A.; Ray, P. C. *ACS Nano* **2007**, *1*, 208–214.
(20) He, X.; Liu, H.; Li, Y.; Wang, S.; Li, Y.; Wang, N.; Xiao, J.; Xu, X.; Zhu, D. *Adv. Mater.* **2005**, *17*, 2811–2815.
(21) Lin, S. Y.; Liu, S. W.; Lin, C. M.; Chen, C. H. *Anal. Chem.* **2002**, *74*, 330–335.
(22) Scampicchio, M.; Lawrence, N. S.; Arecchi, A.; Mannino, S. *Electroanalysis* **2007**, *19*, 2437–2443.
(23) Fatkins, D. G.; Zheng, W. *Anal. Biochem.* **2008**, *372*, 82–88.
(24) Zaborska, W.; Karcz, W.; Kot, M.; Juszkiewicz, A. *Food Chem.* **2009**, *112*, 42–45.
(25) Frens, G. *Nat. Phys. Sci.* **1973**, *241*, 20–22.
(26) Ji, X.; Song, X.; Li, J.; Bai, Y.; Yang, W.; Peng, X. *J. Am. Chem. Soc.* **2007**, *129*, 13939–13948.
(27) Chen, Y. M.; Yu, C. J.; Cheng, T. L.; Tseng, W. L. *Langmuir* **2008**, *24*, 3654–3660.
(28) Storhoff, J. J.; Elghanian, R.; Mucic, R. C.; Mirkin, C. A.; Letsinger, R. L. *J. Am. Chem. Soc.* **1998**, *120*, 1959–1964.

AM9001953